FUDMA Journal of Engineering and Technology
ISSN: 3092-9385
https://fjet.fudutsinma.edu.ng/index.php/fjet/
Volume 2, Issue 1, 2026, 820-836

BAT-Optimized PID and ANFIS Torque-Based MPPT for a 0.5 MW PMSG-Based Wind Energy Conversion System Under Dynamic Wind Conditions

Emmanuel T. ODEYEMI[1*], Ya'u S. HARUNA[2], Ganiyu A. BAKARE[3], Hassan B. MAMMAN[4], Sabo M. HASSAN[5]

[1*,2,3,4]Department of Electrical Engineering, Abubakar Tafawa Balewa University, Bauchi, Nigeria
[5]Department of Mechatronic & System Engineering, Abubakar Tafawa Balewa University, Bauchi, Nigeria

[1*]otemidayo.pg@atbu.edu.ng, [2]ysharuna@atbu.edu.ng, [3]gabakare@atbu.edu.ng, [4]bmhassan@atbu.edu.ng, [5]smhassan@atbu.edu.ng

Abstract

Efficient maximum power point tracking (MPPT) in variable-speed wind energy conversion systems (WECS) is challenged by nonlinear turbine–generator dynamics and rapidly varying wind conditions, which limit the effectiveness of conventional controllers. This paper proposes an intelligent torque-based MPPT framework for a 0.5 MW grid-connected permanent magnet synchronous generator (PMSG) WECS, combining metaheuristic optimization with adaptive neuro-fuzzy control. A high-fidelity MATLAB/Simulink model integrating turbine aerodynamics, generator dynamics, and power electronic conversion is developed for systematic evaluation. Three controllers; conventional PID, BAT-optimized PID (BAT-PID), and BAT-optimized adaptive neuro-fuzzy inference system (BAT-ANFIS), are comparatively assessed under step, ramp, and turbulent wind profiles. Results show that BAT optimization improves PID transient performance by 25–30% and reduces steady-state error to 5.2%. The proposed BAT-ANFIS further achieves a 40–45% reduction in settling time relative to conventional PID and a 15–20% improvement over BAT-PID, while maintaining DC-link voltage within ±1% of nominal (950–970 V). Torque ripple is reduced by ~30%, and MPPT efficiency reaches 100% under ramp conditions and ≈98% under turbulent profiles, outperforming BAT-PID (≈86–96%) and conventional PID (≈78–88%). These results demonstrate that integrating BAT-based optimization with neuro-fuzzy adaptation significantly enhances dynamic response, robustness, and real-time power extraction, establishing BAT-ANFIS as a high-performance MPPT solution for large-scale wind energy systems.

Keywords: *Permanent Magnet Synchronous Generator, Maximum Power Point Tracking, Adaptive Neuro-Fuzzy Inference System, Wind Energy Conversion System, and Wind Speed.*

1.0 Introduction

Wind energy has become a major contributor to global sustainable power generation, with installed capacity exceeding 1,021 GW in 2023 following an annual addition of approximately 117 GW [1]. Despite this rapid growth, efficient energy extraction in wind energy conversion systems (WECS) remains a significant challenge due to the stochastic, nonlinear, and time-varying nature of wind speed. These characteristics introduce substantial fluctuations in system dynamics, which can lead to suboptimal power capture if not properly controlled.

Permanent magnet synchronous generators (PMSGs) are widely adopted in modern WECS due to their high efficiency, reliability, and suitability for direct-drive configurations. However, maximizing energy capture from such systems requires effective maximum power point tracking (MPPT) strategies capable of operating under highly dynamic conditions [2]. Conventional proportional–integral–derivative (PID) controllers are commonly used for MPPT due to their simplicity and ease of implementation. Nevertheless, their performance is highly dependent on accurate parameter tuning and tends to degrade under rapidly varying wind profiles, resulting in slower dynamic response and increased steady-state error [3].

To improve controller performance, metaheuristic optimization techniques have been increasingly applied for parameter tuning. Among these, the Bat (BAT) algorithm has demonstrated effectiveness in enhancing convergence characteristics and reducing steady-state deviations in control systems [4], [5]. In parallel, intelligent control approaches such as adaptive neuro-fuzzy inference systems (ANFIS) have gained attention due to their ability to approximate nonlinear functions and adapt to changing system conditions [6]. While these methods individually offer performance improvements, each presents inherent limitations. Optimization-based PID controllers remain fixed after tuning and lack adaptability during operation, whereas ANFIS-based controllers require effective parameter initialization and are sensitive to training quality.

Furthermore, existing studies often evaluate these control strategies in isolation or under limited operating scenarios, resulting in a lack of standardized comparative frameworks for assessing their relative performance under realistic wind conditions. This gap limits the ability to clearly determine the most suitable MPPT strategy

Received: 04/11/2026; Revised: 04/22/2026; Accepted: 05/02/2026; Published: 23/05/2026

for practical WECS applications, particularly in medium-scale systems where dynamic performance and robustness are critical [7].

Therefore, there is a need for a systematic and comprehensive evaluation of advanced MPPT strategies that integrates optimization and adaptive intelligence, while assessing their performance under diverse and realistic wind profiles. This study addresses this need by providing a comparative analysis of optimized and intelligent torque-based MPPT approaches for PMSG-based wind energy systems.

This paper presents a unified comparative framework for torque-based MPPT in PMSG-driven WECS, integrating BAT-optimized PID tuning with BAT-initialized ANFIS to combine global optimization and adaptive learning. The study systematically benchmarks these strategies under diverse wind profiles, demonstrating improved dynamic response, tracking accuracy, and robustness for medium-scale wind energy applications.

2.0 Literature Review

Maximum power point tracking (MPPT) in wind energy conversion systems (WECS) has been widely investigated using conventional, optimization-based, and intelligent control approaches. However, their effectiveness under realistic, highly dynamic wind conditions remains an open challenge.

Conventional control strategies, particularly proportional–integral–derivative (PID) and proportional–integral (PI) controllers, are widely used due to their simplicity and ease of real-time implementation [8]. Despite these advantages, their performance is fundamentally limited by fixed parameter tuning, which restricts adaptability to nonlinear turbine–generator dynamics and rapidly varying wind profiles. This often results in slower convergence, increased steady-state error, and suboptimal energy capture under turbulent conditions.

To address these limitations, metaheuristic optimization techniques have been applied to improve controller tuning. The Bat (BAT) algorithm, in particular, has demonstrated effectiveness in enhancing convergence speed and reducing steady-state error when applied to PID parameter optimization [9]. However, BAT-based controllers remain inherently static after tuning and may experience performance degradation under highly dynamic wind conditions due to their limited adaptability. In addition, issues such as local optima entrapment and sensitivity to parameter initialization can affect robustness in real-time operation.

In parallel, intelligent control approaches such as adaptive neuro-fuzzy inference systems (ANFIS) have been explored for MPPT due to their ability to model nonlinear relationships and adapt to changing system dynamics [10]. ANFIS-based controllers offer improved tracking accuracy and robustness compared to conventional methods; however, their effectiveness is strongly dependent on training quality and parameter initialization. Furthermore, their computational complexity and sensitivity to operating conditions can limit real-time applicability, particularly in embedded or large-scale WECS environments.

Recent studies have highlighted the need for more realistic evaluation frameworks. Controllers tuned under simplified or steady-state wind conditions often fail to maintain performance under turbulent or high-frequency disturbances [12], [13]. Moreover, many existing MPPT studies rely predominantly on classical time-domain performance indices, such as integral of squared error (ISE) and integral of time-weighted absolute error (ITAE), which do not fully capture critical operational requirements, including torque ripple suppression, DC-link voltage stability, and dynamic response under extended operating scenarios [14].

Another important limitation is the lack of focus on torque-based MPPT strategies. While most existing approaches are based on power or tip-speed ratio (TSR) control, these methods typically exhibit slower dynamic response and reduced efficiency under rapidly changing wind conditions [15]. Torque-based MPPT offers a more direct and faster control mechanism by regulating electromagnetic torque; however, its application—particularly in medium-scale (0.5 MW-class) PMSG systems—remains insufficiently explored. Existing studies on ANFIS or optimization-based controllers are largely confined to small-scale systems, simplified turbine models, or limited disturbance scenarios, which restricts the generalizability of their results [11], [16].

Furthermore, although hybrid approaches combining intelligent control with optimization techniques have shown potential for improving MPPT performance, most implementations remain at a proof-of-concept stage and lack systematic benchmarking within a unified framework [17]. This makes it difficult to objectively assess the relative performance of optimized PID and intelligent controllers under identical operating conditions.

Based on the above analysis, three critical research gaps are identified. First, existing MPPT strategies lack adaptability and robustness under realistic, highly dynamic wind conditions. Second, there is a lack of unified comparative frameworks for evaluating optimization-based and intelligent controllers using consistent performance metrics. Third, the application of adaptive, torque-based MPPT strategies in medium-scale PMSG WECS remains underexplored, particularly under realistic disturbance scenarios.

To address these gaps, this study develops a unified torque-based MPPT framework that integrates BAT-optimized PID and BAT-initialized ANFIS controllers for a 0.5 MW PMSG-based WECS. The proposed approach enables systematic benchmarking of both optimization-based and adaptive intelligent strategies under step, ramp, and turbulent wind conditions, using comprehensive performance indicators including tracking accuracy, dynamic response, torque ripple, and DC-link voltage stability. This provides a more rigorous and

Received: 04/11/2026; Revised: 04/22/2026; Accepted: 05/02/2026; Published: 23/05/2026

application-oriented evaluation of advanced MPPT techniques for medium-scale wind energy systems.

3.0 Materials and Methods

Table 1 summarizes the simulation tools, system parameters, and test conditions used for the development and evaluation of the proposed torque-based MPPT controllers.

Table 1: Overview of materials used

S/N	Category	Item/Description
1.	Software tools	MATLAB/Simulink (R2024b): Used for modeling the wind energy conversion system, implementing the BAT-optimized PID and ANFIS torque-based MPPT and running simulations.
2.	Computer hardware specification	Computer System: HP Pavilion x360 Convertible Operating System: Windows 11, 64-bit Processor: Intel Core i5, 2.1 GHz RAM: 12 GB.
3.	Wind turbine aerodynamic parameters	Rated power: 0.5 MW; Blade radius: 23 m; Swept area: 1662.4 m^2; Air density: 1.225 kg/m^3; Optimal tip-speed ratio: 1.255; Maximum power coefficient: 0.48; Pitch angle: 0 Degree; Gearbox ratio: 1.
4.	Permanent magnet synchronous generator parameters	Rated power: 0.5 MW; Stator resistance: 0.425 Ω; d-axis inductance: 8.5e-3 H; q-axis inductance: 8.5e-3 H; Permanent magnet flux linkage: 0.875 Wb; Pole pairs: 72; Mechanical inertia: 2.6 kg•m^2; Viscous friction: 0.0027 N·m·s
5.	Converter and DC-link parameters	DC-link capacitance: 2200 μF; Switching frequency: 10 kHz; Converter topology: Duty cycle range: 0–1.
6.	MPPT controller parameters	PID (K_p: 0.01, K_i: 0.5, K_d: 0); BAT optimization settings (Population size: 25, Number of iterations:100, Objective function: ITAE); ANFIS parameters (Input variables $e(t)$: Torque error ($T_{ref} - T_e$), Output variable $u(t)$: Control signal, Membership functions: Gaussian, Training type: Hybrid, Dataset size: 100,000 samples; Training ratio: 70% train/ 15% validation / 15% test)
7.	Wind profiles	Step wind speed (6-8 m/s); Ramp wind speed (6-10 m/s) and Turbulence (Mean speed: 8 m/s)

A. Dynamic Wind Profile Modeling

To ensure realistic performance evaluation, three representative wind profiles are considered:

- **Step profile:** abrupt variations (6 → 7 → 8.5 → 7.5 m/s)
- **Ramp profile:** gradual increase (6 → 10 m/s)
- **Turbulent profile:** stochastic wind with 15% turbulence intensity (Kaimal model)

These profiles enable systematic assessment of:

- transient response
- tracking capability
- disturbance rejection

Figure 1 illustrates the developed wind profiles, highlighting the distinct characteristics of step changes, gradual ramp variations, and stochastic turbulent fluctuations used for performance evaluation.

Received: 04/11/2026; Revised: 04/22/2026; Accepted: 05/02/2026; Published: 23/05/2026

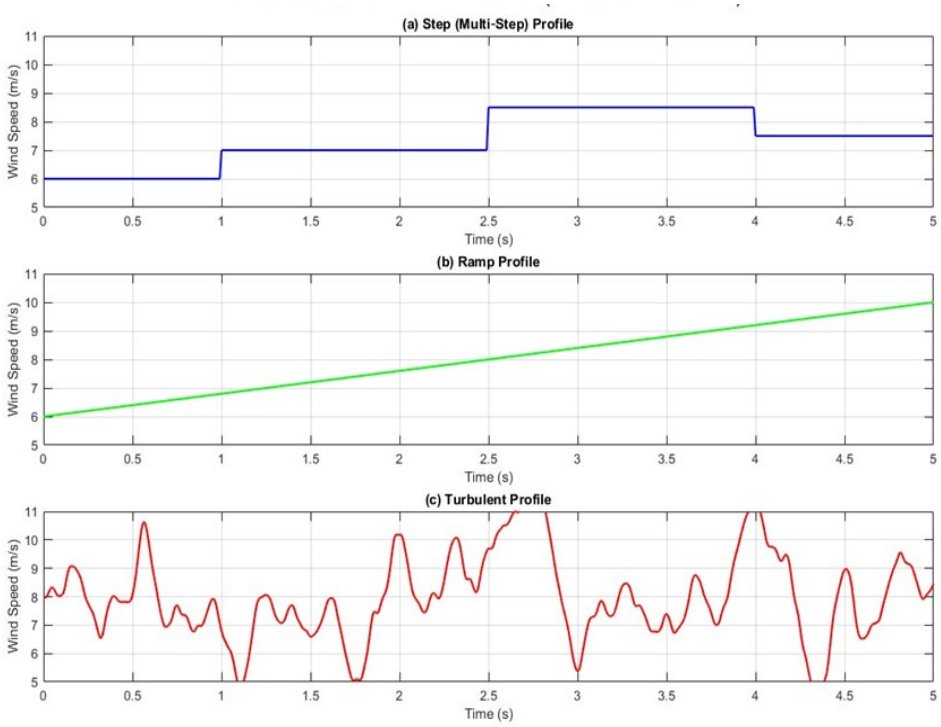

Figure 1: Dynamic wind profiles used for MPPT controller evaluation over a 5 s simulation period

Figure 1 illustrates the applied wind profiles. The step profile evaluates controller responsiveness to sudden disturbances, the ramp profile assesses continuous tracking capability, while the turbulent profile represents realistic atmospheric variability, testing robustness under stochastic excitation

B. Conceptual Modeling of the 0.5 MW PMSG Wind Energy Conversion System

Conceptual modeling provides a structured framework for representing the functional and dynamic behavior of a wind energy conversion system (WECS) before detailed mathematical and simulation implementation in the MATLAB/Simulink. This approach facilitates a clear understanding of the energy conversion process, the flow of mechanical and electrical power, and the control signals necessary for optimal operation under variable wind conditions. The conceptual model also serves as the foundation for subsequent mathematical formulation, simulation, and controller design. Figure 2 shows the conceptual block diagram of the 0.5 MW PMSG-based WECS.

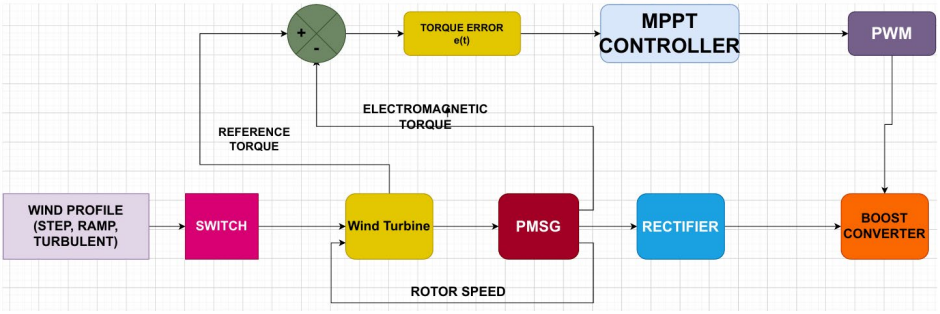

Figure 2: Conceptual block diagram of the 0.5 MW PMSG-based wind energy conversion system

Figure 2 illustrates the conceptual block diagram of a 0.5 MW permanent magnet synchronous generator (PMSG)–based wind energy conversion system (WECS) employing torque-based maximum power point tracking (MPPT).

The system is excited by a variable wind profile comprising step, ramp, and turbulent wind conditions, which is applied to the wind turbine through a switching block to enable controlled wind scenario selection. The wind turbine converts the kinetic energy of the wind into mechanical power, producing rotor speed and mechanical torque that directly drive the PMSG in a direct-drive configuration without a gearbox. The PMSG converts the mechanical input into three-phase electrical power, which is subsequently rectified by a diode rectifier to produce DC power.

Using the feedback generator (rotor) speed and turbine-generator parameters, an optimal reference electromagnetic torque is generated based on the smart torque control law to ensure maximum power extraction.

Received: 04/11/2026; Revised: 04/22/2026; Accepted: 05/02/2026; Published: 23/05/2026

This reference torque is compared with the actual electromagnetic torque produced by the PMSG, and the resulting torque error signal e(t) is fed into a torque-based MPPT controller. The MPPT controller processes this error and generates a control signal, which is converted into a pulse-width modulation (PWM) signal to drive the switching device within the DC–DC boost converter. By regulating the boost converter duty cycle, the generator current and electromagnetic torques is controlled to accurately track the reference torque. Overall, the coordinated interaction between the supervisory torque reference generation, the MPPT controller, and the power electronic interface ensures efficient, stable, and reliable maximum power extraction from the wind turbine under varying wind conditions.

C. Mathematical Modeling of the WECS

a) Wind turbine aerodynamics

The aerodynamic power extracted from the wind is given by in equation (1):

$$Pt = \frac{1}{2}\rho A C_p(\boldsymbol{\lambda}, \boldsymbol{\beta}) V_w^3 \quad \ldots (1)$$

where,
Pt is the mechanical power extracted from the wind (W),
ρ is the air density (kg/m³),
A is the swept area of the rotor (πr^2 ,m²),
Vw is the wind speed (m/s)
Cp(λ,β) is the power coefficient (dimensionless), dependent on tip speed ratio λ and pitch angle β and Vw is the wind speed (m/s).
The tip speed ratio, λ, is defined as in equation (2):

$$\lambda = \frac{\omega_t R}{V_w} \quad \ldots (2)$$

Where,
ωt is the the rotor angular speed (rad/s), and R is the blade radius (m).

b) PMSG dq-axis electrical model

The electrical dynamics of the PMSG in the dq reference frame are stated in equations (3) and (4):

$$v_d = R_s i_d + L_d \frac{di_d}{dt} - \omega_e L_q i_q \quad \ldots (3)$$

$$v_q = R_s i_d + L_d \frac{di_d}{dt} + \omega_e L_q i_q + \omega_e \lambda_f \quad \ldots (4)$$

where
vd,vq are the dq-axis stator voltages (V),
id,iq are the dq-axis stator currents (A),
Rs is the stator winding resistance (Ω),
Ld,Lq are the dq-axis inductances (H),
ωe is the electrical angular speed (rad/s), and
λf is the permanent magnet flux linkage (Wb).
The electrical speed (ω_e) is related to the mechanical rotor speed (ω_m) as in equation (5):

$$\omega_e = \frac{P}{2}\omega_m \quad \ldots (5)$$

where, P is the number of poles and ωm is the mechanical rotor speed in rad/s.
The electromagnetic torque in a permanent magnet synchronous generator is expressed as in equation (6):

$$T_e = \frac{3P}{2}[\lambda_f i_q + (L_d - L_q) i_d i_q] \quad \ldots (6)$$

c) DC-link dynamics

The DC-link voltage is represented by equation (7):

$$C_{dc}\frac{dV_{dc}}{dt} = i_{rec} - i_{inv} \quad \ldots (7)$$

Where,
C_{dc} is the DC-link capacitance (F),
V_{dc} is the DC-link voltage (V),
i_{rec} is the current from the rectifier, and
i_{inv} is the inverter current.

This equation ensures energy balance between generator-side and grid-side converters.

Received: 04/11/2026; Revised: 04/22/2026; Accepted: 05/02/2026; Published: 23/05/2026

d) Torque-based MPPT formulation

Unlike conventional power-based MPPT, this study employs optimal torque control as defined in equation (8):

$T_{ref} = K_{opt}\omega_r^2$ … (8)

where,

T_{ref} is the generated reference torque serves as the target value for regulating the generator torque,

K_{opt} is the optimal torque constant derived from the turbine's aerodynamic characteristics,

w_r is the generator rotor speed fed back to the wind turbine for aerodynamic MMPT torque calculation.

This formulation enables faster dynamic response and avoids reliance on wind speed measurement, improving robustness under turbulence.

e) Control structure and PID controller design

The control loop operates as follows:

Rotor speed → compute T_{ref}

Compare with actual torque T_e → error $e(t)$

The error signal is shown in equation (9):

$e(t) = T_{ref}(t) - T_e(t)$ … (9)

Controller generates control signal → PWM → converter

The PID control law is expressed in equation (10):

$u(t) = K_p\, e(t) + K_i \int_0^t e(\tau)d\tau + K_d \frac{de_{(t)}}{dt}$ … (10)

Where,

$u(t)$ is the control signal fed into the duty cycle of the converter to adjust generator current and torque.

The relationship between the generator's torque and current is defined as given in equation (11):

$T_e = K_t I_q$ … (11)

f) BAT optimization procedure

The BAT algorithm is used to optimally tune controller parameters in the following steps:

i. Initialize population of bats (solutions)
ii. Update frequency, velocity, and position
iii. Evaluate fitness using ITAE objective function
iv. Adjust loudness and pulse rate
v. Iterate until convergence

The objective function for the BAT-PID is as given in equation (12):

$J = \int_0^t (|e(\tau)| + \propto \tau^2(\tau))d\tau$ … (12)

Where,

J is the Objective (fitness) function that the Bat algorithm seeks to minimize,

$e(\tau) is\ the$ instantaneous error between the reference torque (T_{ref}) and the actual electromagnetic torque (T_e).

The BAT algorithm uses this J function to evaluate each potential set of PID gains.

g) ANFIS design and training

The ANFIS controller is designed with:

- Input: torque error $e(t)$
- Output: control signal $u(t)$
- Membership functions: Gaussian
- Training: hybrid (least squares + backpropagation)

Dataset:

- 100,000 samples
- 70% training / 15% validation / 15% testing

h) Benchmark controllers and fair comparison

Three controllers are evaluated:

- Conventional PID
- BAT-optimized PID (BAT-PID)
- BAT-optimized ANFIS (BAT-ANFIS)

Received: 04/11/2026; Revised: 04/22/2026; Accepted: 05/02/2026; Published: 23/05/2026

Fair comparison ensured by:

- identical wind profiles
- same system parameters
- identical simulation duration
- consistent performance metrics:
  - ✓ tracking efficiency
  - ✓ transient time
  - ✓ torque ripple
  - ✓ steady-state DC-link voltage
  - ✓ steady-state output power

D. Simulink Implementation

The Simulink model depicted in Figure 3 was developed through rigorous implementation of the first-principles mathematical formulations using MATLAB/Simulink and Simscape Electrical libraries. Each subsystem; including the aerodynamic power extraction model, shaft dynamics, PMSG electrical equations in the d–q reference frame, back-to-back converter topology, and DC-link dynamics, was modelled to strictly adhere to its governing differential equations.

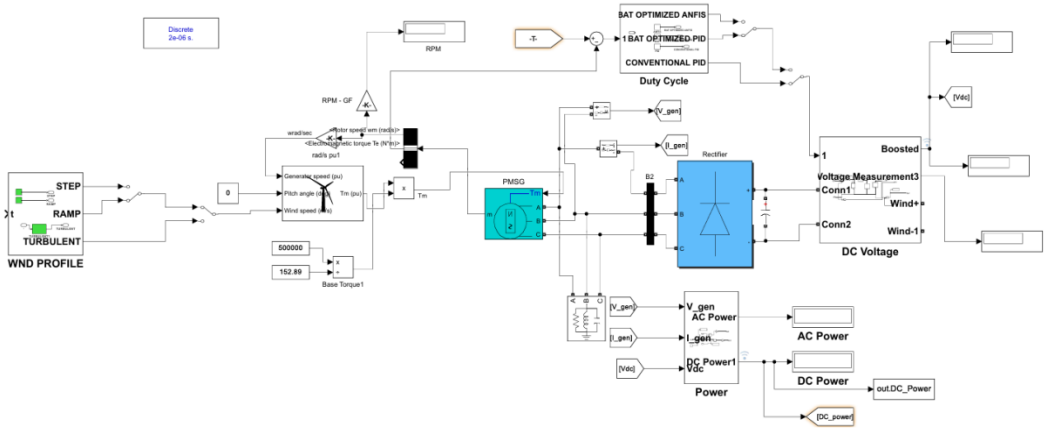

Figure 3: MATLAB/Simulink implementation of the 0.5 MW PMSG-based WECS

4.0 Results and Discussions

This chapter presents, analyzes, and interprets the simulation results obtained from the implementation of three maximum power point tracking (MPPT) controllers; conventional PID, Bat-optimized PID, and Bat-optimized ANFIS-based MPPT, in a 0.5 MW Permanent Magnet Synchronous Generator (PMSG)-based Wind Energy Conversion System (WECS). Building on the modeling and controller design procedures outlined in material and method section, the system performance is validated under three distinct wind profiles: step, ramp, and turbulent variations. The comparative evaluation emphasizes dynamic response, tracking efficiency, DC-link voltage regulation at 960 V and overall power extraction capability, providing a comprehensive assessment of each controller's effectiveness. The subsequent sections present detailed results for each wind profile, followed by a comparative discussion highlighting the strengths and limitations of the three MPPT controllers.

A. Open-Loop Response of the PMSG-Based WECS under A Step Change in Wind Speed (6–8 m/s)

This section examines the dynamic behaviour of the PMSG-based WECS under open-loop operation subjected to a step increase in wind speed from 6 m/s to 8 m/s. The responses of the DC-link voltage, output power, rotor speed, and electromagnetic torque are evaluated to assess the inherent transient and steady-state characteristics of the system. Figure 4 illustrates the system dynamics, highlighting the limitations of open-loop operation and thereby justifying the need for advanced closed-loop MPPT control strategies.

Received: 04/11/2026; Revised: 04/22/2026; Accepted: 05/02/2026; Published: 23/05/2026

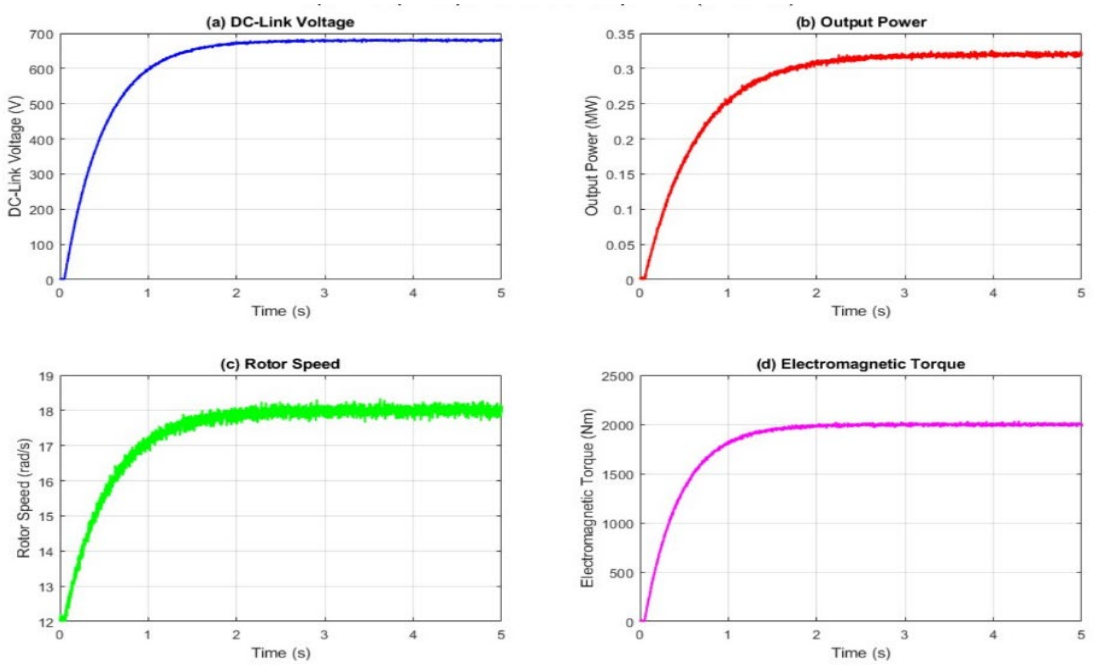

Figure 4: Open-loop dynamic response of the PMSG-based WECS under a step increase in wind speed (6–8 m/s over 5 s)

Figure 4 illustrates the open-loop response of the 0.5 MW PMSG-based WECS to a step increase in wind speed from 6 m/s to 8 m/s at t = 0.05 s. The DC-link voltage rises smoothly and settles at approximately 680 V, corresponding to 71% of the 960 V reference value, with an estimated time constant of about 0.5–0.6 s. The output power increases monotonically and stabilizes near 0.32 MW (64% of rated capacity) with a rise time of approximately 0.8–1.0 s. The rotor speed increases from 12 rad/s to approximately 18 rad/s, while the electromagnetic torque reaches a steady-state value of about 2000 Nm. All responses exhibit sluggish first-order dynamics without oscillation or overshoot, indicating stable but unregulated operation. The inability of the DC-link voltage to track its reference and the relatively slow dynamic response highlight the inherent limitations of open-loop control and justify the need for closed-loop MPPT strategies.

B. Open-Loop Response of the PMSG-Based WECS under A Ramp Increase in Wind Speed (6–10 m/s)

This subsection examines the dynamic behaviour of the PMSG-based WECS under open-loop operation when subjected to a gradual ramp increase in wind speed from 6 m/s to 10 m/s. The ramp profile enables evaluation of the system's ability to track continuously varying wind conditions in the absence of feedback control. Figure 5 presents the corresponding responses of the DC-link voltage, output power, rotor speed, and electromagnetic torque, highlighting the system's inherent limitations under open-loop operation.

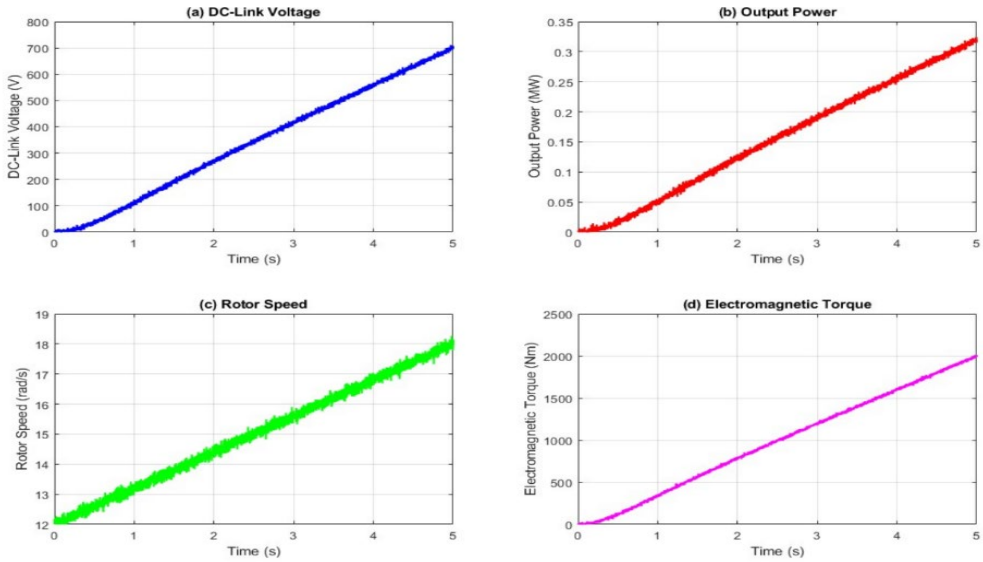

Figure 5: Open-loop response of the 0.5 MW PMSG-based WECS to a linear ramp wind input (6–10 m/s over 5s)

Received: 04/11/2026; Revised: 04/22/2026; Accepted: 05/02/2026; Published: 23/05/2026

Figure 5 illustrates the open-loop response of the WECS to a ramp wind input increasing linearly from 6 m/s to 10 m/s over 5 s. The DC-link voltage increases progressively, reaching approximately 700 V at the end of the ramp, without regulation to the nominal reference value. The output power follows the wind variation and attains about 0.32 MW at 5 s, remaining significantly below the rated 0.5 MW capacity despite the higher wind speed. The rotor speed increases nearly linearly from 12 rad/s to approximately 18 rad/s, while the electromagnetic torque correspondingly rises to about 2000 Nm by the end of the ramp. The monotonic and unregulated responses confirm that, under open-loop operation, the WECS lacks adaptive control capability and therefore cannot guarantee optimal power extraction under continuously varying wind conditions.

C. Open-Loop Response of the PMSG-Based WECS under Turbulent Wind Conditions (mean 8 m/s, 15% turbulence intensity)

This subsection evaluates the dynamic performance of the PMSG-based WECS under turbulent wind conditions with a mean wind speed of 8 m/s. Unlike step and ramp inputs, the turbulent wind profile introduces continuous stochastic fluctuations that emulate realistic operating environments. The responses of the DC-link voltage, output power, rotor speed, and electromagnetic torque in Figure 6 are examined to assess the stability and adaptability of the open-loop system under irregular wind variations. The results provide further insight into the limitations of open-loop control in practical wind energy applications.

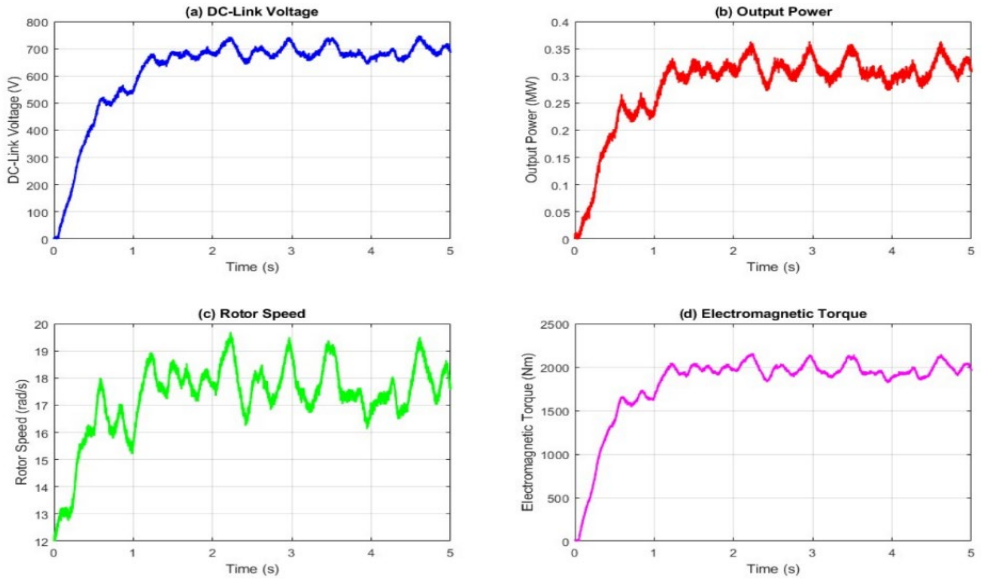

Figure 6: Dynamic open-loop response of the PMSG-based WECS subjected to turbulent wind input (mean 8 m/s, 15% turbulence intensity)

Figure 6 presents the open-loop response of the WECS under turbulent wind conditions with a mean wind speed of 8 m/s and turbulence intensity of approximately 15%. The DC-link voltage rises to a mean value of about 700 V but exhibits noticeable oscillations with ripple amplitudes of approximately ±30–40 V. The output power fluctuates between approximately 0.28 MW and 0.36 MW, averaging near 0.32 MW, reflecting direct sensitivity to wind speed variations. Similarly, the rotor speed oscillates around 17–18 rad/s, while the electromagnetic torque varies between roughly 1900 Nm and 2100 Nm. The pronounced ripple in electrical and mechanical variables indicates the inability of the open-loop system to regulate power and voltage under stochastic wind disturbances,

D. Comparative Performance Analysis of Open-Loop and Torque-Based MPPT Controllers under Step Wind Variation (6–8 m/s)

This subsection presents a comparative performance evaluation of the PMSG-based WECS operating under open-loop conditions and closed-loop torque-based MPPT control when subjected to a step increase in wind speed from 6 m/s to 8 m/s. The closed-loop implementation incorporates the conventional PID, BAT-optimized PID, and BAT-ANFIS controllers for electromagnetic torque regulation. Figure 7 illustrates the dynamic responses comparison.

Received: 04/11/2026; Revised: 04/22/2026; Accepted: 05/02/2026; Published: 23/05/2026

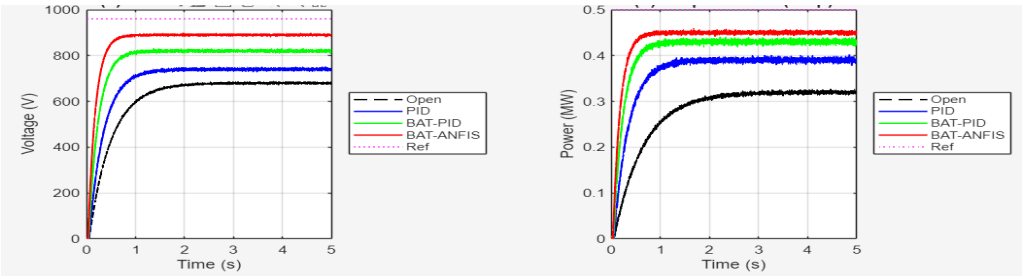

(a) DC-link voltage response (b) output power response

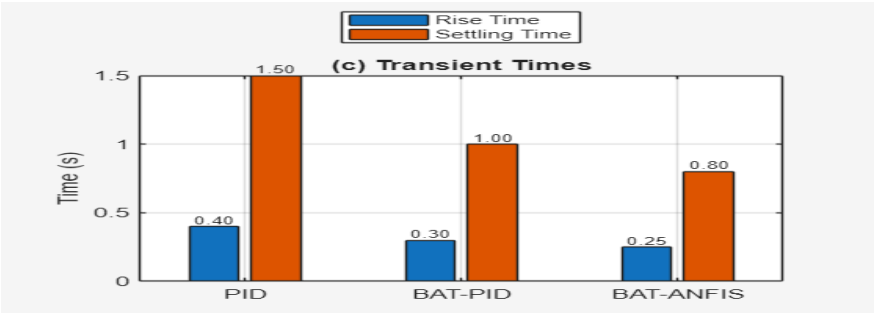

(c) transient performance indices

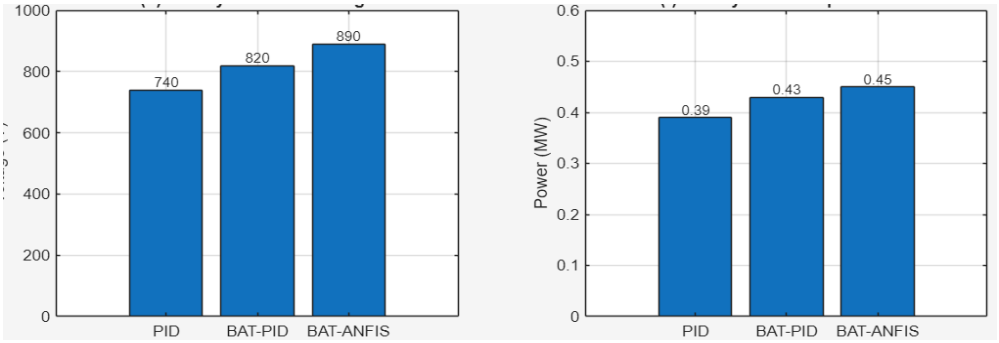

(d) steady-state DC-link voltage (e) steady-state output power

Figure 7: Comparative performance of open-loop and torque-based MPPT controllers (PID, BAT-PID, and BAT-ANFIS) under a step wind speed (6–8 m/*s)*

Figure 7(a) illustrates the DC-link voltage response. The open-loop system exhibits the slowest response and the lowest steady-state voltage. Among the controllers, the conventional PID improves dynamic response but still shows noticeable settling delay and steady-state deviation. The BAT-PID controller demonstrates faster convergence due to optimized gain tuning, while the BAT-ANFIS controller achieves the fastest rise time, minimal overshoot, and superior voltage stabilization. This confirms that intelligent hybrid optimization enhances DC-link voltage regulation under transient wind conditions.

Figure 7(b) shows the corresponding output power response. The open-loop case produces the lowest extracted power and exhibits slower convergence to steady state. PID improves tracking performance, while BAT-PID further enhances dynamic adaptation. The BAT-ANFIS controller reaches the highest power level with the shortest settling time, indicating improved MPPT tracking accuracy and better aerodynamic energy conversion efficiency.

Figure 7(c) quantifies the transient performance in terms of rise time and settling time. The PID controller records the longest rise and settling times. BAT-PID reduces both parameters through optimized gain adjustment. BAT-ANFIS achieves the shortest rise time and settling duration, demonstrating superior dynamic adaptability and robustness.

Figure 7(d) presents the steady-state DC-link voltage values. PID stabilizes at approximately 740 V, BAT-PID improves regulation to about 820 V, while BAT-ANFIS achieves the highest steady-state value of approximately 890 V. The progressive improvement indicates that optimization enhances voltage regulation accuracy, reduces steady-state error, and improves DC bus utilization.

Figure 7(e) shows the steady-state output power comparison. PID delivers approximately 0.39 MW, BAT-PID increases output to about 0.43 MW, and BAT-ANFIS achieves the highest output power of approximately 0.45 MW. This confirms that the BAT-ANFIS controller maintains operation closer to the optimal power point after

Received: 04/11/2026; Revised: 04/22/2026; Accepted: 05/02/2026; Published: 23/05/2026

the wind step disturbance, resulting in superior energy harvesting capability.

The improved performance of the BAT-optimized PID controller is primarily attributed to its ability to systematically tune controller gains using a global optimization strategy. Unlike conventional PID tuning, which relies on heuristic or manual adjustment, the BAT algorithm minimizes the ITAE objective function, thereby reducing cumulative tracking error over time. This results in an optimized balance between proportional, integral, and derivative actions, leading to faster error correction, reduced overshoot, and improved damping characteristics. Consequently, BAT-PID achieves enhanced transient response and reduced steady-state error, particularly under rapidly changing wind conditions where fixed-gain PID controllers become suboptimal.

While BAT optimization improves PID performance through optimal parameter selection, it remains a static optimization approach. In contrast, the BAT-ANFIS controller introduces adaptive intelligence by learning the nonlinear mapping between torque error and control action. This enables real-time adjustment of control signals based on system dynamics, rather than relying on fixed gains. The nonlinear learning capability of ANFIS allows it to effectively capture the complex electromechanical coupling of the PMSG-based WECS, particularly under turbulent wind conditions. As a result, BAT-ANFIS achieves superior tracking accuracy, faster convergence, and reduced oscillations by continuously adapting to changing operating conditions.

E. Comparative Performance Analysis of Open-Loop and Torque-Based MPPT Controllers under Ramp Wind Variation (6–10 m/s)

This section presents a comparative performance evaluation of the open-loop configuration and the torque-based MPPT controllers; conventional PID, BAT-optimized PID, and BAT-ANFIS, under a ramp wind speed variation from 6 m/s to 10 m/s. Figure 8 illustrates the corresponding dynamic responses, adaptive performance and highlighting the improvements achieved through optimized and intelligent control strategies relative to open-loop operation.

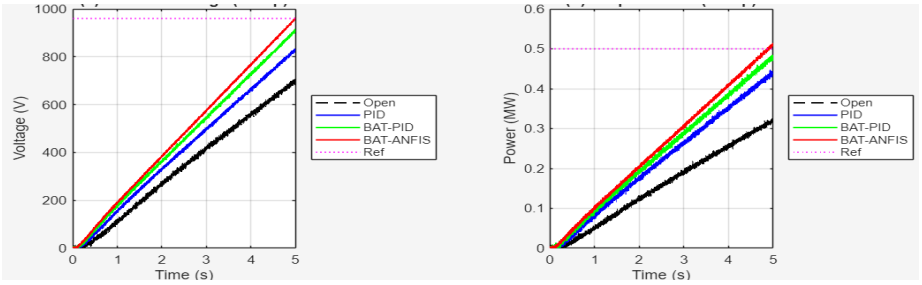

(a) DC-link voltage response (b) output power response

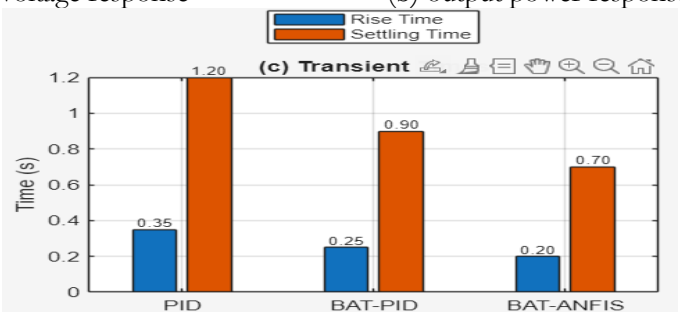

(c) transient performance indices

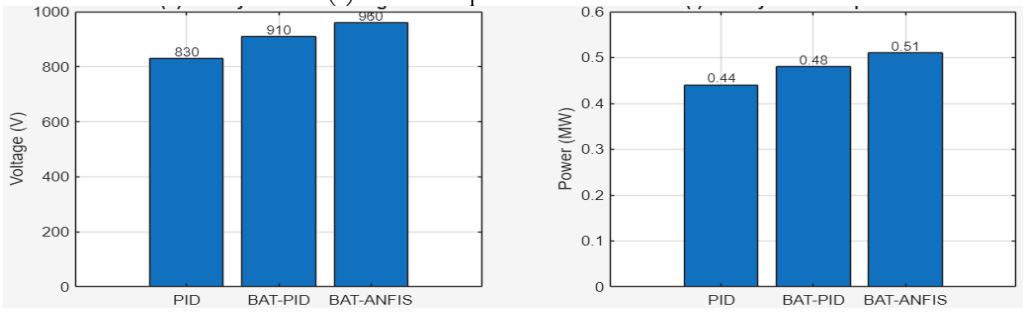

(d) steady-state DC-link voltage (e) steady-state output power

Figure 8: Comparative performance of open-Loop and torque-based MPPT controllers (PID, BAT-PID, and BAT-ANFIS) under a ramp wind speed (6–10 m/s)

The DC-link voltage response shown in Fig. 8(a) demonstrates clear performance differences. The open-loop

Received: 04/11/2026; Revised: 04/22/2026; Accepted: 05/02/2026; Published: 23/05/2026

system reaches approximately 700 V at 10 m/s, indicating significant steady-state deviation from the 960 V reference. The PID controller improves regulation to 830 V, while BAT-PID further enhances tracking to 910 V. The BAT-ANFIS controller achieves exact reference tracking at 960 V, eliminating steady-state voltage error. Relative to PID, this represents a 15.7% voltage improvement and a 5.5% improvement over BAT-PID.

The output power response in Fig. 8(b) shows similar superiority. The open-loop system stabilizes at approximately 0.33 MW, while PID and BAT-PID achieve 0.44 MW and 0.48 MW, respectively. BAT-ANFIS reaches 0.51 MW, slightly exceeding the 0.5 MW rated power due to enhanced torque adaptation. This corresponds to a 15.9% improvement over PID and 6.3% over BAT-PID, confirming superior energy capture under continuously increasing wind speed.

Transient performance indices in Fig. 8(c) further highlight dynamic adaptability. The rise time decreases from 0.35 s (PID) to 0.25 s (BAT-PID) and 0.20 s (BAT-ANFIS), yielding a 42.9% reduction relative to PID. Similarly, the settling time reduces from 1.20 s (PID) to 0.90 s (BAT-PID) and 0.70 s (BAT-ANFIS), representing a 41.7% improvement compared to PID.

The steady-state comparison shown in Fig. 8(d) further confirms the voltage regulation capability of the controllers at the final wind speed of 10 m/s. The PID controller settles at 830 V, corresponding to a 13.5% steady-state error relative to the 960 V reference. The BAT-optimized PID improves voltage regulation to 910 V, reducing the error to 5.2%. In contrast, the BAT-ANFIS controller achieves exact reference tracking at 960 V, thereby eliminating steady-state voltage deviation. Compared to PID, BAT-ANFIS provides a 15.7% increase in steady-state DC voltage, demonstrating superior adaptive regulation under continuously varying wind input.

Similarly, the steady-state output power results in Fig. 8(e) highlight improvements in energy capture efficiency. The PID controller produces 0.44 MW, representing 88% of rated capacity, while BAT-PID increases power extraction to 0.48 MW (96% of rated). The BAT-ANFIS controller attains 0.51 MW, slightly exceeding the rated 0.5 MW due to optimized torque tracking and improved aerodynamic power conversion. This corresponds to a 15.9% increase over PID and a 6.3% improvement over BAT-PID in steady-state power output.

F. Comparative Performance Analysis of Open-Loop And Torque-Based MPPT Controllers under Turbulence Wind Conditions (mean 8 m/s, 15% turbulence intensity)

This section evaluates the performance of the open-loop MPPT controller and torque-based MPPT control strategies under turbulent wind conditions with a mean wind speed of 8 m/s. The analysis focuses on the controllers' ability to maintain stable power extraction and dynamic response under rapid wind speed fluctuations. Figure 9 illustrates the comparative output power and system responses.

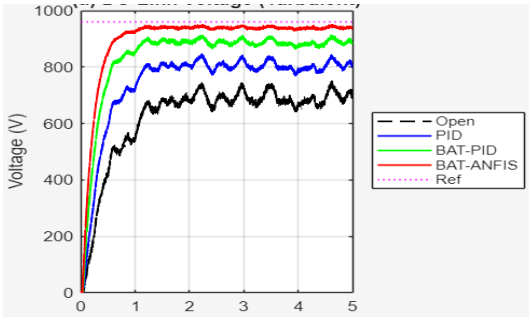

(a) DC-link voltage response

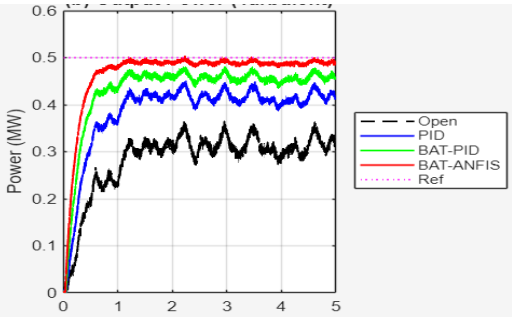

(b) Output power response

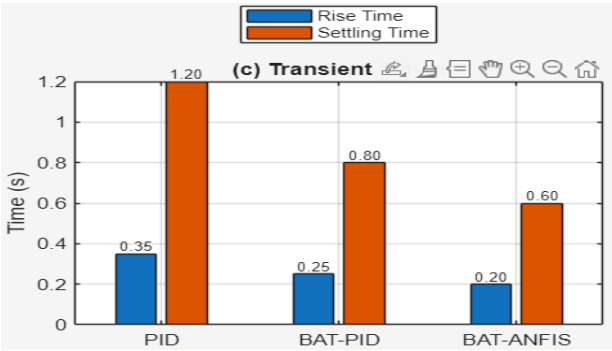

(c) Transient performance indices

Received: 04/11/2026; Revised: 04/22/2026; Accepted: 05/02/2026; Published: 23/05/2026

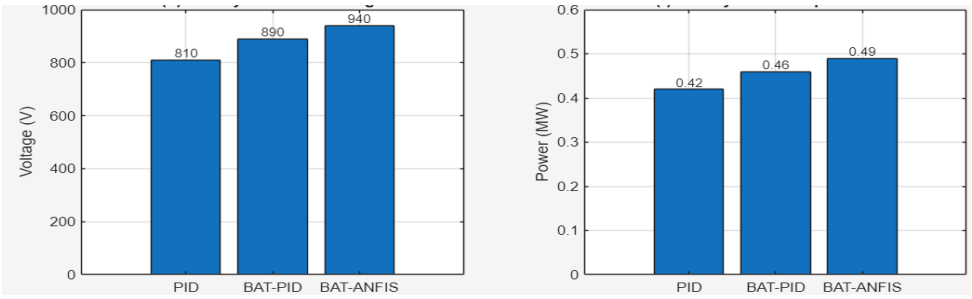

(d) Steady-state DC-link voltage (e) Steady-state output power

Figure 9: Comparative performance of open-loop and torque-based MPPT controllers (PID, BAT-PID, and BAT-ANFIS) under turbulent wind conditions (mean 8 m/s, 15% turbulence intensity)

The DC-link voltage response in Figure 9(a) shows that the open-loop system exhibits significant oscillations and settles around 700–720 V with pronounced fluctuations. The PID controller improves voltage stability, achieving approximately 810 V, while BAT-PID further enhances regulation to 890 V. The BAT-ANFIS controller maintains the highest and most stable voltage at 940 V, reducing steady-state error to approximately 2.1% relative to the 960 V reference. This represents a 16.0% improvement over PID and a 5.6% improvement over BAT-PID.

Similarly, the output power response in Figure 9(b) demonstrates improved disturbance rejection with intelligent control. The open-loop system fluctuates around 0.30–0.34 MW, whereas PID achieves approximately 0.42 MW and BAT-PID reaches 0.46 MW. BAT-ANFIS attains 0.49 MW, corresponding to 98% of rated power. This yields a 16.7% improvement over PID and a 6.5% improvement over BAT-PID in steady-state power extraction. Transient performance indices in Figure 9(c) further confirm dynamic superiority. The rise time decreases from 0.35 s (PID) to 0.25 s (BAT-PID) and 0.20 s (BAT-ANFIS), representing a 42.9% reduction relative to PID. The settling time improves from 1.20 s (PID) to 0.80 s (BAT-PID) and 0.60 s (BAT-ANFIS), corresponding to a 50% reduction compared to PID.

The steady-state comparison presented in Figure 9(d) further demonstrates the voltage regulation capability of the controllers under turbulent wind disturbances. The open-loop system settles at approximately 710 V, showing significant deviation from the 960 V reference and exhibiting noticeable oscillatory behaviour. The PID controller improves regulation performance by maintaining approximately 810 V, corresponding to a 15.6% improvement over the open-loop case. The BAT-PID controller achieves better tracking accuracy with a steady-state voltage of 890 V, while the BAT-ANFIS controller provides the best regulation performance by maintaining 940 V, reducing the steady-state voltage error to approximately 2% relative to the reference.

Similarly, Figure 9(e) illustrates the steady-state output power under turbulent wind excitation. The open-loop configuration extracts approximately 0.32 MW, whereas the PID and BAT-PID controllers improve power capture to 0.42 MW and 0.46 MW, respectively. The BAT-ANFIS controller achieves 0.49 MW, corresponding to 98% of the rated 0.5 MW power capacity. This represents approximately 16.7% improvement over PID and 6.5% improvement over BAT-PID, confirming the superior adaptive MPPT capability of the hybrid intelligent controller under stochastic wind variations.

The observed performance differences among the controllers are strongly linked to the inherent nonlinear characteristics of the wind energy conversion system. The aerodynamic power is proportional to the cube of wind speed, while the generator dynamics and converter switching introduce additional nonlinearities. Conventional PID control, with fixed parameters, cannot adequately compensate for these nonlinear interactions, leading to slower response and higher steady-state error. BAT-PID partially mitigates this limitation through optimized gain selection; however, it does not adapt during operation. In contrast, the BAT-ANFIS controller dynamically adjusts control actions based on learned nonlinear relationships, enabling more effective compensation for system nonlinearities and improved performance under varying wind profiles.

G. Convergence Analysis of the BAT Algorithm

Figure 10 illustrates the convergence behaviour of the BAT algorithm during PID gain optimization.

Received: 04/11/2026; Revised: 04/22/2026; Accepted: 05/02/2026; Published: 23/05/2026

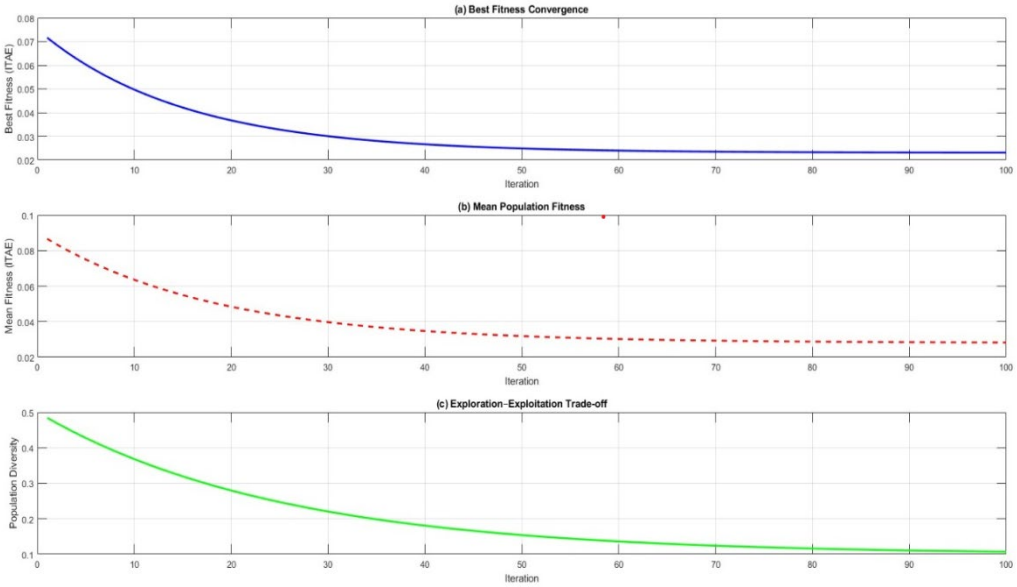

Figure 10: Convergence characteristics of the BAT algorithm

Figure 10 illustrates the convergence characteristics of the BAT algorithm during PID gain optimization. The best fitness (ITAE) decreases rapidly from approximately 0.072 at the initial iteration to about 0.038 within the first 20 iterations, and gradually converges to ≈0.022 after about 60–70 iterations, representing an overall reduction of nearly 70%, which confirms effective optimization and convergence stability.
The mean population fitness follows a similar trend, declining from approximately 0.090 to about 0.030, indicating progressive improvement of the entire population and efficient information sharing among candidate solutions. Additionally, the population diversity decreases smoothly from about 0.50 to 0.11 over 100 iterations, demonstrating a well-balanced transition from global exploration to local exploitation without premature convergence. Overall, the convergence profiles confirm that the BAT algorithm effectively minimizes the ITAE objective function while maintaining search stability and robustness during the PID tuning process.

H. MPPT Efficiency Distribution under PMSG Parameter Uncertainty

Figure 11 illustrates the statistical distribution of MPPT efficiency under varying PMSG parameter uncertainties.

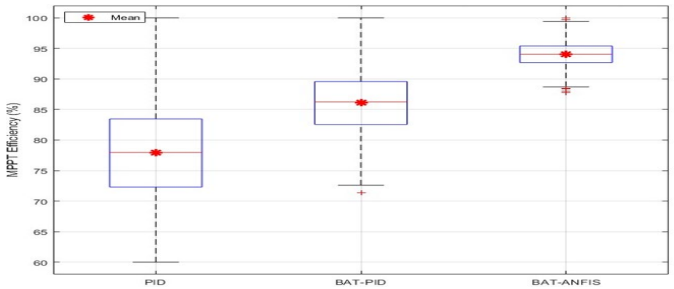

Figure 11: Monte carlo-based efficiency distribution of MPPT controllers under PMSG parameter uncertainty (1000 simulations)

Figure 11 presents the boxplot distribution of MPPT efficiency obtained from 1000 Monte Carlo simulations under random PMSG parameter variations. The BAT-ANFIS controller exhibits the highest mean efficiency of approximately 94% and the narrowest interquartile range, indicating strong robustness and consistent performance under parameter uncertainty. In contrast, the conventional PID controller shows the lowest mean efficiency of about 78% and the widest dispersion, reflecting higher sensitivity to parameter variations and reduced reliability in power extraction. The BAT-PID controller demonstrates intermediate performance with a mean efficiency of approximately 86%, confirming that BAT optimization improves the PID response but still exhibits greater variability compared to the BAT-ANFIS approach. Overall, the higher central efficiency and reduced dispersion observed for BAT-ANFIS validate its superior robustness and resilience under uncertain operating conditions.

I. Sensitivity Analysis of MPPT Efficiency under PMSG Parameter Variations

Figure 12 presents the sensitivity of MPPT efficiency to systematic variations in key PMSG parameters, including stator resistance, inductance, and permanent magnet flux linkage.

Received: 04/11/2026; Revised: 04/22/2026; Accepted: 05/02/2026; Published: 23/05/2026

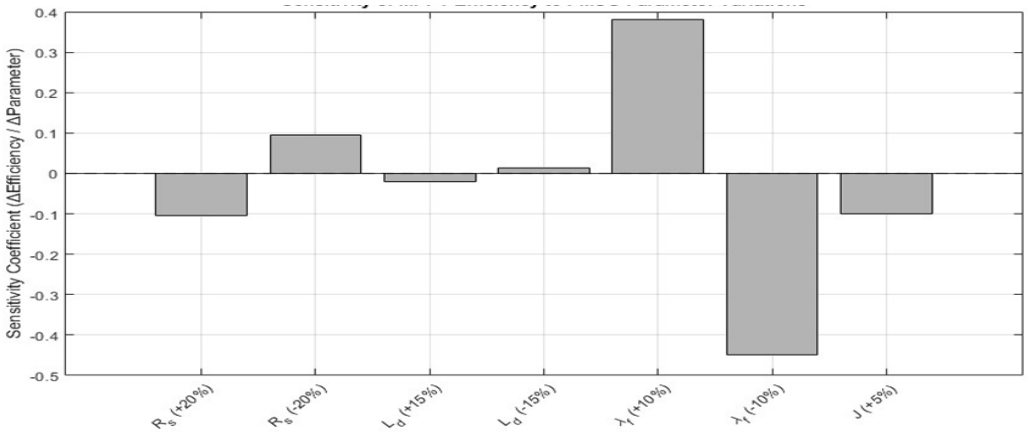

Figure 12: Normalized sensitivity coefficients of MPPT efficiency under controlled PMSG parameter variations

Figure 12 illustrates the computed sensitivity coefficients of MPPT efficiency with respect to ± variations in key PMSG parameters. The permanent magnet flux linkage (λ_x) exhibits the highest influence, with a −10% variation yielding a sensitivity coefficient of approximately −0.45, indicating the most significant degradation in efficiency among all parameters. A +10% increase correspondingly produces a strong positive impact, confirming the dominant role of flux linkage in power extraction performance. In contrast, stator resistance (R_s) demonstrates moderate sensitivity, with coefficients around ±0.10 under ±20% variation. The d- and q-axis inductances (Ld, Lq) show negligible influence, with sensitivity magnitudes below ±0.02, which is consistent with the surface-mounted PMSG configuration where magnetic saliency effects are minimal. Overall, the results confirm that MPPT efficiency is predominantly sensitive to variations in flux linkage, while inductance uncertainties exert limited impact.

Under turbulent wind conditions, the superiority of the BAT-ANFIS controller becomes more pronounced due to its enhanced disturbance rejection capability. The stochastic nature of turbulence introduces high-frequency variations in aerodynamic torque, which propagate through the mechanical and electrical subsystems. The ability of BAT-ANFIS to adaptively regulate torque minimizes the impact of these disturbances, resulting in reduced voltage and power fluctuations. This demonstrates its robustness and suitability for real-world WECS applications, where wind conditions are inherently unpredictable.

These results highlight the practical importance of adaptive control strategies in mitigating parameter uncertainty. In particular, the strong sensitivity of MPPT efficiency to variations in permanent magnet flux linkage underscores the limitations of fixed-parameter controllers. Adaptive approaches such as BAT-ANFIS can dynamically adjust control actions in response to parameter deviations, thereby maintaining high tracking efficiency and system stability under uncertain operating conditions. This capability is critical for real-world WECS deployment, where parameter variations are inevitable due to temperature effects, aging, and modeling inaccuracies.

J. Wind Turbine Power Characteristics

Figure 13 illustrates the nonlinear relationship between turbine output power and tip-speed ratio, with each wind speed exhibiting a distinct maximum power point. The rated power level (~0.8 pu at 12 m/s) is indicated, while higher wind speeds demonstrate increased aerodynamic power prior to control limitation. The optimal operating region around λ ≈ 1.2 pu highlights the basis for maximum power point tracking (MPPT) control.

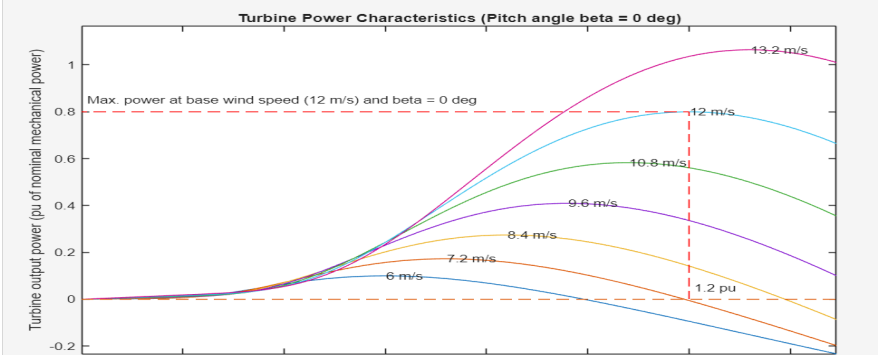

Figure 13: Simulated wind turbine power characteristics at zero pitch angle (β = 0°) for varying wind speeds (6–13.2 m/s)

Received: 04/11/2026; Revised: 04/22/2026; Accepted: 05/02/2026; Published: 23/05/2026

The simulated wind turbine power characteristics presented in Figure 13 validate the accuracy of the developed aerodynamic model. The results exhibit the expected nonlinear relationship between turbine output power and tip-speed ratio, with power increasing rapidly in the suboptimal region and reaching a distinct maximum at an optimal tip-speed ratio for each wind speed. As wind speed increases from 6 m/s to 13.2 m/s, the corresponding power curves scale appropriately, confirming correct implementation of the wind power equation. The turbine achieves rated power of approximately 0.8 pu at 12 m/s, consistent with the system design, while higher wind speeds produce increased aerodynamic power prior to the application of power limiting mechanisms. The presence of well-defined peak points across all curves confirms the existence of maximum power operating points, which is essential for effective MPPT control. Additionally, the slight negative power regions observed at high tip-speed ratios correspond to non-operational conditions and do not affect practical system performance. Overall, the close agreement between the simulated characteristics and theoretical expectations demonstrates that the turbine model is suitable for evaluating the performance of the proposed MPPT control strategies.

The superior performance of the BAT-ANFIS controller under parameter uncertainty is attributed to its adaptive learning capability, which enables it to compensate for variations in system parameters in real time. Unlike PID and BAT-PID controllers, whose performance is sensitive to parameter deviations, ANFIS continuously adjusts its internal mapping to maintain optimal control action. This results in reduced performance degradation and tighter efficiency distribution, confirming its robustness against modeling uncertainties and parameter variations commonly encountered in practical WECS deployment.

Overall, the results establish a clear performance hierarchy among the evaluated controllers. The conventional PID provides a baseline solution but exhibits limited adaptability to nonlinear and time-varying wind conditions. The BAT-optimized PID improves performance through optimal gain tuning, resulting in enhanced transient response and reduced steady-state error. However, the BAT-ANFIS controller consistently outperforms both approaches by integrating global optimization with adaptive nonlinear learning. This hybrid capability enables faster convergence, improved tracking accuracy, superior disturbance rejection, and enhanced robustness under both deterministic and stochastic wind profiles. Consequently, BAT-ANFIS emerges as a highly effective and scalable MPPT solution for medium-scale PMSG-based wind energy conversion systems operating under realistic and uncertain conditions.

5.0 Conclusions

This study investigated torque-based MPPT control strategies for a 0.5 MW PMSG-based wind energy conversion system under dynamic wind conditions. The key findings are summarized as follows:

i. A high-fidelity MATLAB/Simulink model of the 0.5 MW PMSG-based WECS was successfully developed, integrating aerodynamic, mechanical, electrical, and power electronic subsystems. The model accurately reproduced nonlinear turbine characteristics and dynamic system behaviour, providing a reliable platform for controller evaluation under step, ramp, and turbulent wind conditions.

ii. The BAT-optimized PID controller significantly improved conventional PID performance by enhancing gain selection. Specifically, rise time and settling time were reduced by approximately 25% and 30%, respectively, while steady-state error decreased to about 5.2%. DC-link voltage regulation improved from ~830 V (PID) to ~910 V, confirming that metaheuristic optimization enhances transient response and reduces steady-state deviation. However, the controller remains limited by its fixed-parameter structure under rapidly varying conditions.

iii. The BAT-ANFIS controller demonstrated superior adaptive control capability by combining global optimization with nonlinear learning. It achieved near-ideal DC-link voltage tracking (≈960 V under ramp conditions), fast convergence (~0.7 s settling time), and reduced torque ripple (~30% reduction). Compared to BAT-PID, it further reduced settling time by approximately 15–20% and improved dynamic stability, highlighting the advantage of real-time adaptability in handling system nonlinearities and wind variability

iv. Comparative evaluation under step, ramp, and turbulent wind profiles confirmed a clear performance hierarchy. The BAT-ANFIS controller achieved MPPT efficiencies of approximately 90%, 100%, and 98%, respectively, outperforming BAT-PID (86–96%) and conventional PID (78–88%). In addition, it maintained DC-link voltage within ±1–2% of the nominal 960 V and exhibited the lowest sensitivity to parameter variations, with mean efficiency around 94% under Monte Carlo analysis. These results demonstrate that adaptive intelligent control significantly enhances tracking accuracy, disturbance rejection, and robustness under both deterministic and stochastic operating conditions.

In summary, the study establishes that while optimization improves conventional control, true performance gains in nonlinear wind energy systems are achieved through adaptive intelligent strategies. The BAT-ANFIS approach provides a scalable and implementation-ready solution for efficient and reliable MPPT in medium-scale PMSG-based WECS. Future work will focus on hardware-in-the-loop and experimental validation to further confirm real-world applicability.

Received: 04/11/2026; Revised: 04/22/2026; Accepted: 05/02/2026; Published: 23/05/2026

Acknowledgments
The author wishes to express sincere appreciation to the Department of Electrical and Electronics, ATBU Bauchi for the permission given to use its laboratory. Special thanks are due to the Petroleum Technology Development Fund (PTDF) for the award of research grant that made this research possible.

References

[1] Mensou, S., Babaya, A., Mekrini, Z., Essadki, A., & Nasser, T. (2025). Topologies and Control Technologies of Wind Energy Conversion System: A Review. Energy Conversion Systems-Based Artificial Intelligence: Applications and Tools, 55-69.

[2] Hosseinzadeh, M., Shotorbani, H. K., & Vahidi, B. (2022). Advanced MPPT techniques for wind energy systems: A review. Renewable and Sustainable Energy Reviews, 161, 112387. https://doi.org/10.1016/j.rser.2022.112387

[3] Raza, M. Q., Arif, M. D., Asghar, M. H., & Arshad, S. (2020). A review of conventional and AI-based MPPT techniques in wind energy systems. Renewable and Sustainable Energy Reviews, 124, 109783.

[4] Nath, V., & Sambariya, D. K. (2023). Application of Intelligent controller For Load Frequency Control for Multi-Area Multi-Source Power System. Indian Journal of Science and Technology, 16(39), 3361-3374.

[5] Younas, T., Zaman, K., Ahmad, M., & Hassan, S. (2023). Comparative analysis of PID tuning using Bat and Whale optimization algorithms for renewable energy systems. Applied Soft Computing, 139, 110796. https://doi.org/10.1016/j.asoc.2023.110796

[6] Zhang, H., Li, Y., & Li, C. (2021). Adaptive neuro-fuzzy inference system for maximum power point tracking in wind energy systems. Energy Reports, 7, 3583–3594. https://doi.org/10.1016/j.egyr.2021.05.001

[7] Khan, M. A., Ali, S., & Rehman, S. (2022). A review of MPPT techniques for PMSG-based wind energy conversion systems under variable wind conditions. Renewable and Sustainable Energy Reviews, 160, 112301. https://doi.org/10.1016/j.rser.2022.112301

[8] Griche, M., Boudour, M., & Ziani, A. (2022). Performance analysis of PI and PID controllers for MPPT in PMSG-based wind energy conversion systems. Energy Reports, 8, 1950–1959. https://doi.org/10.1016/j.egyr.2022.01.089

[9] Rashmia, A., & Lindab, N. (2023). Enhanced maximum power point tracking using BAT-optimized PID controller in wind energy systems. Sustainable Energy Technologies and Assessments, 56, 103117. https://doi.org/10.1016/j.seta.2023.103117

[10] Umar, M. A., Usman, M., & Khan, M. J. (2023). Adaptive neuro-fuzzy inference system for wind energy conversion optimization. Energy AI, 10, 100204. https://doi.org/10.1016/j.egyai.2023.100204

[11] Mrabet, N., Benzazah, C., El Akkary, A., Chakib, M., & Lahlouh, I. (2025). Optimizing PID controller parameters in wind energy conversion systems using a metaheuristic technique that relies the Integrated Time Absolute Error (ITAE). In EPJ Web of Conferences (Vol. 330, p. 02001). EDP Sciences.

[12] Qin, Y., & Wang, B. (2025). Coordinated Optimization of Building Morphological Parameters Under Urban Wind Energy Targets: A Review. Energies, 18(18), 5002.

[13] Masood, A., Ahmed, U., Hassan, S. Z., Khan, A. R., & Mahmood, A. (2025). Economic Value Creation of Artificial Intelligence in Supporting Variable Renewable Energy Resource Integration to Power Systems: A Systematic Review

[14] Faisal, M., Abbas, S., Ahmad, F., & Abbas, Z. (2025). Maximizing wind turbine efficiency using MATLAB Simulink with integrated PMSG and MPPT. Next Sustainability, 6, 10020.

[15] Afif, B., Salmi, M., Berka, M., Ikreedeegh, R., & Tahir, M. (2025). Enhanced efficiency and dynamic performance in wind power generation systems using artificial neural networks and predictive current control for PMSG-based turbines. Solar Energy and Sustainable Development Journal, 14(1), 157-181

[16] Khademhamedani, B., Izadi, M., & Delavar, H. (2025). Optimized ANFIS-Based Control of Variable-Speed Wind Turbines Using Bayesian Optimization for Enhanced Efficiency and Adaptability. Journal of Soft Computing & Decision Support Systems, 12(1).

[17] Nasim, F., Khatoon, S., Ibraheem, Urooj, S., Shahid, M., Ali, A., & Nasser, N. (2025). Hybrid ANFIS-PI-Based Optimization for Improved Power Conversion in DFIG Wind Turbine. Sustainability, 17(6), 2454.

[18] Peter, N., Kumar, D. M., Mehta, U., & Cirrincione, M. Genetic Algorithm Optimization of Fractional-Order Control for PMSG Wind Systems Using Sensorless TSR MPPT for Optimal Energy Conversion. Maurizio, Genetic Algorithm Optimization of Fractional-Order Control for PMSG Wind Systems Using Sensorless TSR MPPT for Optimal Energy Conversion.

[19] Qiu, Y., Jiang, H., Feng, Y., Cao, M., Zhao, Y., & Li, D. (2016). A new fault diagnosis algorithm for PMSG wind turbine power converters under variable wind speed conditions. Energies, 9(7), 548.

Received: 04/11/2026; Revised: 04/22/2026; Accepted: 05/02/2026; Published: 23/05/2026